Color Image Deblurring with Impulsive Noise

Leah Bar[1], Alexander Brook[2], Nir Sochen[3], and Nahum Kiryati[1]

[1] School of Electrical Engineering, Tel-Aviv University, Israel
[2] Dept. of Mathematics, Technion, Israel
[3] Dept. of Applied Mathematics, Tel-Aviv University, Israel

Abstract. We propose a variational approach for deblurring and impulsive noise removal in multi-channel images. A robust data fidelity measure and edge preserving regularization are employed. We consider several regularization approaches, such as Beltrami flow, Mumford-Shah and Total-Variation Mumford-Shah. The latter two methods are extended to multi-channel images and reformulated using the Γ-convergence approximation. Our main contribution is in the unification of image deblurring and impulse noise removal in a multi-channel variational framework. Theoretical and experimental results show that the Mumford-Shah and Total Variation Mumford Shah regularization methods are superior to other color image restoration regularizers. In addition, these two methods yield a denoised edge map of the image.

1   Introduction

Image deblurring and denoising are classical problems that have been extensively studied. Consider the standard linear and space invariant blur model with additive noise. Let z denote the blurred and noisy image, h the blur kernel, u the original image and n the noise. Thus, $z = h * u + n$. In the multi-channel case,

$$z^{\sigma} = h^{\sigma} * u^{\sigma} + n^{\sigma},$$

where σ indicates the channel. In the processing of standard color images, $\sigma \in \{r, g, b\}$. We assume that $h^{\sigma} = h$ for all σ. This approximation holds for cameras with lenses of reasonable quality.

Consider first the single-channel case. A variational approach to the recovery of u from z (given h) is based on the minimization of a cost functional that includes fidelity and regularization terms. The fidelity term quantifies the discrepancy between the observed image z and the blurred version $h * u$ of the recovered image. The regularization term is necessary since the image deconvolution problem is ill-posed.

The fidelity terms in variational image deblurring methods are commonly designed for Gaussian noise and are thus based on the L^2 norm

$$\int (h * u - z)^2 \ dA \ .$$

To better deal with outliers and impulsive noise in image deconvolution, fidelity measurement using the L^1 norm

$$\int |h * u - z| \, dA$$

can be considered. In practice, the modified L^1 norm

$$\int \sqrt{(h * u - z)^2 + \eta} \, dA$$

is an approximation that offers numerical advantages ($0 < \eta \ll 1$).

Regularization in variational image deblurring can be accomplished using various stabilizers, such as Tikhonov (L^2) [1], Total Variation (L^1) [2–4] and ϕ-formalism [5, 6]. Recently, elements of the Mumford-Shah functional have been used for regularization in the image deblurring problem [7].

Deblurring of color images in the variational framework has received surprisingly little attention. Blomgren and Chan [8] extended the Total Variation norm to vector-valued images in the context of image denoising. Barash [9] restored color images by combining an L^2 fidelity term with Perona-Malik regularization [10], but processed each channel separately. Two recent studies on color image deblurring were presented by Welk *et al* [6] and Kaftory *et al* [11]. The former study used L^2 fidelity terms and a coupled multi-channel extension of the Perona-Malik regularizer. The latter presented a color image deblurring method employing an L^2 fidelity term and Beltrami flow regularization. Other than in the variational framework, multispectral Wiener-based restoration was suggested in [12]; see also [13, 14].

This research concentrates on the deblurring of multi-channel images contaminated by impulsive noise. Addressing the problem in the variational setting, we extend the L^1 fidelity measure to multi-channel images. We study several regularization terms, and propose the generalization of two efficient stabilizers to the multi-channel case. The novel cost functionals, algorithms and theoretical discussions are supported by comparative experiments. Successful color image deblurring at high levels of impulse noise is demonstrated.

2   Cost functionals

Image deblurring is an ill-posed inverse problem, that has to be regularized. In the variational framework, the recovered image is the minimizer of a cost functional. In the multi-channel case, the functional is of the general form

$$\mathcal{F} = \int_\Omega \sum_\sigma \Phi(h * u^\sigma - z^\sigma) \, dA + \mathcal{J}(u),$$

where $\Phi(\cdot)$ is a potential function and $\mathcal{J}(u)$ is a regularization operator that depends on all the channels. Ω is the image domain and $u : \Omega \to [0, 1]^3$. In the case of Gaussian noise, a quadratic form of the data-fidelity is appropriate,

$$\Phi(h * u^\sigma - z^\sigma) = (h * u^\sigma - z^\sigma)^2.$$

The quadratic form is inadequate for impulsive noise. To effectively suppress outliers, a (modified) robust L^1 norm can be used [4, 3, 15]:

$$\Phi(h * u^\sigma - z^\sigma) = \sqrt{(h * u^\sigma - z^\sigma)^2 + \eta},$$

where $\eta \ll 1$ is a positive constant.

This study focuses on color image deblurring with impulsive noise. We therefore base the fidelity term, in all the methods we consider, on the multi-channel modified L^1 norm. The methods differ in the regularization used; we present and discuss several possibilities, and evaluate their resulting restoration performance.

Total Variation (TV) regularization, first introduced by Rudin et al [2], has been widely used in image processing. A straightforward but naive extension to color images is via channel-by-channel TV regularization. For each channel,

$$\mathcal{J}^{TV}(u^\sigma) = \beta \int_\Omega |\nabla u^\sigma| \, dA.$$

Channel-by-channel image deblurring, with multiple decoupled functionals, is simple but may lead to artifacts. Specifically, since the channels are decoupled, color edges in different channels may not coincide, resulting in thin false stripes [16]. Channel coupling in TV regularization (Color-TV) was presented by Blomgren and Chan [8].

An alternative approach is the Beltrami flow introduced by Sochen et al [17]. Its superiority with respect to Color-TV regularization has been shown by Tschumperle [18]. In the Beltrami framework, a color image (u^r, u^g, u^b) is regarded as a two-dimensional surface embedded in $\mathbb{R}^5$-space spanned by (x, y, u^r, u^g, u^b). The area of this surface is given by

$$\int_\Omega \sqrt{\det G} \, dA,$$

where the metric G takes the form

$$G = \begin{pmatrix} 1 + \gamma^2 \sum_\sigma (u_x^\sigma)^2 & \gamma^2 \sum_\sigma u_x^\sigma u_y^\sigma \\ \gamma^2 \sum_\sigma u_x^\sigma u_y^\sigma & 1 + \gamma^2 \sum_\sigma (u_y^\sigma)^2 \end{pmatrix}.$$

This area is a measure of image smoothness, and has the important advantage of gradient alignment between channels. The Beltrami functional is given by

$$\mathcal{J}^{BEL} = \alpha \int_\Omega \sqrt{\det(G)} \, dA.$$

The advantages of this regularizer are more obvious if we rewrite it as

$$\int_\Omega \sqrt{1 + \gamma^2 \sum_\sigma (|\nabla u^\sigma|^2) + \frac{1}{2}\gamma^4 \sum_{\sigma_1, \sigma_2} |\nabla u^{\sigma_1} \times \nabla u^{\sigma_2}|^2} \, dA,$$

where $\times$ denotes cross-product. The cross-product term enforces channel alignment, making the gradients (u_x^σ, u_y^σ), $\sigma \in \{r, g, b\}$ parallel to each other, and

producing crisp color edges [19]. In the late stages of minimization, when the cross-product term is nearly zero, J^{BEL} approaches the robust Total Variation norm.

Reflecting the preference for piecewise smooth images, parts of the Mumford-Shah segmentation functional [20] can be used for regularization in image restoration as well [7]. In this stabilizer, the energy assigned to a gray level image $u : \Omega \to [0,1]$ with an edge set $K \subset \Omega$ is

$$\mathcal{J}^{MS}(u,K) = \beta \int_{\Omega \setminus K} |\nabla u|^2 dA + \alpha \int_K d\mathcal{H}^1.$$

The first term forces the smoothness of u everywhere except on the discontinuity set K. The second term minimizes the one-dimensional Hausdorff measure (length) of the discontinuity set. Using the Γ-convergence framework, Ambrosio and Tortorelli [21] approximated this irregular functional by a sequence of regular functionals

$$\mathcal{J}_\epsilon^{MS}(u,v) = \beta \int_\Omega v^2 |\nabla u|^2 \ dA + \alpha \int_\Omega \left(\epsilon |\nabla v|^2 + \frac{(v-1)^2}{4\epsilon} \right) \ dA \ . \qquad (1)$$

The auxiliary function $v(x)$ represents the edges. The minimizers of $\mathcal{J}_\epsilon^{MS}$ approach the minimizer of $\mathcal{J}^{MS}$ as $\epsilon \to 0$. In the color version of this functional, suggested by Brook $et\ al$ [16],

$$|\nabla u| = \sqrt{\sum_\sigma \left[(u_x^\sigma)^2 + (u_y^\sigma)^2 \right]} \ . \qquad (2)$$

This term is referred to as the Frobenius norm of ∇u. Note that in this regularizer the edge map v is common for the three channels.

A modified version of the Mumford-Shah functional, in its Γ-convergence approximation, was suggested by Shah [22] for gray-level images:

$$\mathcal{J}_\epsilon^{MSTV}(u,v) = \beta \int_\Omega v^2 |\nabla u| \ dA + \alpha \int_\Omega \left(\epsilon |\nabla v|^2 + \frac{(v-1)^2}{4\epsilon} \right) \ dA. \qquad (3)$$

In this version the L^2 norm of ∇u was replaced by the L^1 norm in the first term. Alicandro $et\ al$ [23] proved the Γ-convergence of this functional to

$$\mathcal{J}^{MSTV} = \beta \int_{\Omega \setminus K} |\nabla u| \ dA + \alpha \int_K \frac{|u^+ - u^-|}{1 + |u^+ - u^-|} d\mathcal{H}^1 \ + \ |D^c u|(\Omega),$$

where u^+ and u^- denote the image values on two sides of the edge set K, $\mathcal{H}^1$ is the one-dimensional Hausdorff measure and $D^c u$ is the Cantor part of the distributional derivative Du. This functional was generalized by Brook $et\ al$ [16] for color images where the Frobenius norm (2) was used in this case as well.

In this research, we consider color image deblurring functionals with a multi-channel L^1 fidelity term, and one of the regularization terms $\mathcal{J}^{BEL}$, $\mathcal{J}^{MS}$, and $\mathcal{J}^{MSTV}$. As a baseline, the channel-by-channel $\mathcal{J}^{TV}$ term will also be discussed.

3   Minimization

Minimization of the cost functionals is carried out using the Euler-Lagrange (E-L) equations with homogeneous Neumann boundary conditions $\partial u^\sigma / \partial N = 0$, $\partial v / \partial N = 0$, where N is the normal to the image boundary. We present the E-L equations of the four functionals that we consider. For channel-by-channel TV regularization, the E-L equation is

$$\frac{\delta \mathcal{F}^{TV}}{\delta u^\sigma} = \frac{h * u^\sigma - z^\sigma}{\sqrt{(h * u^\sigma - z^\sigma)^2 + \eta}} * h(-x, -y) - 2\beta \, \nabla \cdot \left(\frac{\nabla u^\sigma}{|\nabla u^\sigma|} \right) \; = \; 0 \quad (4)$$

The Beltrami E-L equation takes the form

$$\frac{\delta \mathcal{F}^{BEL}}{\delta u^\sigma} = \frac{h * u^\sigma - z^\sigma}{\sqrt{(h * u^\sigma - z^\sigma)^2 + \eta}} * h(-x, -y) - \alpha \nabla \cdot \left(\sqrt{\det(G)} G^{-1} \nabla u^\sigma \right) = 0 \, (5)$$

The parameter α can be made adaptive [24]. Here, α is replaced by $\alpha / \sqrt{\det(G)}$ in order to convert the regularizer to the Laplace-Beltrami geometric operator [11].

The objective functionals with the MS and MSTV regularization terms (1,3) depend on the recovered image u and on the edge map v. With MS regularization (1), the E-L equations are

$$\frac{\delta \mathcal{F}_\epsilon^{MS}}{\delta u^\sigma} = \frac{h * u^\sigma - z^\sigma}{\sqrt{(h * u^\sigma - z^\sigma)^2 + \eta}} * h(-x, -y) - 2\beta \nabla \cdot (v^2 \nabla u^\sigma) \; = \; 0 \qquad (6)$$

$$\frac{\delta \mathcal{F}_\epsilon^{MS}}{\delta v} \; = \; 2\beta v |\nabla u|^2 \; + \; \alpha \left(\frac{v-1}{2\epsilon} \right) \; - \; 2\epsilon \, \alpha \nabla^2 v \; = \; 0 \qquad (7)$$

For MSTV regularization (3), the L^1 norm $|\nabla u|$ is replaced by the modified L^1 norm $\sqrt{\gamma + |\nabla u|^2}$. Thus,

$$\frac{\delta \mathcal{F}_\epsilon^{MSTV}}{\delta u^\sigma} = \frac{h * u^\sigma - z^\sigma}{\sqrt{(h * u^\sigma - z^\sigma)^2 + \eta}} * h(-x, -y) - 2\beta \nabla \cdot \left(\frac{v^2 \nabla u^\sigma}{\sqrt{\gamma + |\nabla u|^2}} \right) = 0 \, (8)$$

$$\frac{\delta \mathcal{F}_\epsilon^{MSTV}}{\delta v} = 2\beta v \sqrt{\gamma + |\nabla u|^2} + \alpha \left(\frac{v-1}{2\epsilon} \right) \; - \; 2\epsilon \, \alpha \nabla^2 v \; = \; 0 \qquad (9)$$

It can be easily seen that Eqs. (4,5,6,8) are non-linear integro-differential equations. Following Vogel and Oman [25], linearization of the E-L equations for the color channels u is performed using the fixed point iteration scheme, where their denominators are lagged by one iteration with respect to the numerators. The linearized functions are then solved by the conjugate gradients method. Eqs. (7,9) are linear with respect to v and are solved using the Minimal Residual algorithm. Note that with MS and MSTV regularization, there are four equations to solve. The minimization procedure alternates between u^σ, $\sigma \in \{r, g, b\}$ and v until convergence.

The discretization of $|\nabla u|$ in Eqs. (7) and (9) was carried out using the central difference scheme. Terms of the form $\nabla \cdot (C \, \nabla u^\sigma)$ and $\nabla^2 v$ were discretized using forward difference for the gradient and backward difference for the divergence.

4   Robust Statistics Interpretation

In this section we provide a robust-statistics interpretation of the MS (1) and
MSTV (3) regularizers. Consider half-quadratic regularization [26]. In this ap-
proach, the regularizer is a non-decreasing potential function $\rho(t)$, where in the
context of image restoration $t = |\nabla u|$. A central element in half-quadratic regu-
larization is the representation of ρ as an infimum of a quadratic function with
an auxiliary variable b. Explicitly, if $\rho(\sqrt{t})$ is concave and non-decreasing, we
can write

$$\rho(t) = \inf_b(bt^2 + \Psi(b))$$

such that $\Psi(b)$ is convex and decreasing. This representation is quadratic with
respect to t when b is fixed, and therefore leads to easier optimization. In the
case of edge-preserving image restoration, the auxiliary function b represents the
edges. For example, the Geman and McClure [27] potential function corresponds
to the half-quadratic form

$$\frac{|\nabla u|^2}{1 + |\nabla u|^2/\delta} = b|\nabla u|^2 + \delta(\sqrt{b} - 1)^2,$$

where δ is a positive constant. Teboul $et\ al$ [28] noticed that in the presence of
noise, image restoration requires well-behaved edges. Therefore an edge regular-
ization term $\phi_b(b)$ was added:

$$\mathcal{J} = \lambda_1 \int_\Omega \left[b|\nabla u|^2 + \Psi(b)\right] dA + \lambda_2 \int_\Omega \phi_b(b)dA.$$

In the case that $\Psi(b) = \delta(\sqrt{b} - 1)^2$ and $\phi_b = |\nabla(\sqrt{b})|^2$,

$$\mathcal{J} = \lambda_1 \int_\Omega \left[b|\nabla u|^2 + \delta(\sqrt{b} - 1)^2\right] dA + \lambda_2 \int_\Omega \left|\nabla(\sqrt{b})\right|^2 dA. \tag{10}$$

Substituting $b = v^2$, $\lambda_1 = \beta$, $\delta = \alpha/4\epsilon\beta$ and $\lambda_2 = \alpha\epsilon$ yields equivalence between
Eq. (10) and the MS regularizer (1) in its Γ-convergence approximation. This
regularizer is therefore the robust Geman-McClure ρ function with an additional
spatial edge organization constraint, where

$$\rho^{MS} = \frac{|\nabla u|^2}{1 + |\nabla u|^2/\delta} \tag{11}$$

In the same manner, the robust ρ function that corresponds to the MSTV reg-
ularizer (3) with the modified L^1 norm is ($\delta = \alpha/4\epsilon\beta$)

$$\rho^{MSTV} = \frac{\sqrt{\gamma + |\nabla u|^2}}{1 + \sqrt{\gamma + |\nabla u|^2/\delta}}, \tag{12}$$

with $\delta = \alpha/4\epsilon\beta$.

Fig. 1. Color image deblurring in the presence of impulsive noise, using a multi-channel modified L^1 fidelity term, with four different regularization methods. *Top-left:* Blurred image. *Top-middle:* Blurred image contaminated by 10% salt and pepper noise. *Top-right:* Deblurring with channel-by-channel TV regularization. *Bottom-left:* Beltrami flow. *Bottom-middle:* Color Mumford-Shah (MS). *Bottom-right:* Color TV Mumford-Shah (MSTV).

5 Results

The original 256×256 *Lena* image (not shown) was blurred by a pill-box kernel of radius 3 (7×7 kernel), see Fig. 1 top-left. Each color channel was then contaminated by salt-and-pepper noise of 10% density (top-middle). Image restoration results, with a fidelity term based on the color version of the modified L^1 norm and the various regularization terms are compared in Fig. 1. The modified L^1 norm parameter was set to $\eta = 10^{-4}$ in all experiments. The top-right image is the outcome of the channel-by-channel TV regularization (Eq. 4) with $\beta = 0.1$. Recovery with the Beltrami stabilizer (Eq. 5) is shown bottom left. In this case, the parameters were set to $\alpha = 0.8$ and $\gamma = 0.1$. The images recovered using the MS (Eqs. 6 and 7) and MSTV (Eqs. 8 and 9) regularizers are shown bottom-middle and right respectively. For both methods $\alpha = 0.5$ and $\epsilon = 0.1$, while $\beta = 0.7$ for MS and $\beta = 0.5$ for MSTV.

As can be observed, channel-by-channel TV regularization is inferior with respect to the other three methods. This is not surprising, since channel-by-channel TV regularization does not exploit the inter-channel redundancy. The images recovered using the Beltrami, MS and MSTV stabilizers are of high

Image	10% noise [dB]	30% noise [dB]
Observed	14.96	10.35
TV	21.14	14.8
Beltrami	23.57	21.93
MS	23.87	23.28
MSTV	23.76	23.42

Table 1. PSNR values using several regularization methods

quality, and are quite similar to each other at this moderate noise level. Table 1 (the 10% noise column) provides quantitative comparative evaluation of these deblurring results using PSNR values:

$$\mathrm{PSNR}(I) = 20 \log \sqrt{\frac{3MN}{\sum_\sigma \sum_{i,j} (I_{ij}^\sigma - \hat{I}_{ij}^\sigma)^2}}.$$

Here M and N are the image dimensions, I and $\hat{I}$ are the original and recovered images respectively.

The differences between the Beltrami, MS and MSTV regularizers can be better observed at a higher noise level, see Fig. 2. The blurred *Lena* image, with 30% noise is shown top-left. Shown top-right is the outcome of Beltrami flow regularization with $\alpha = 1.2$ and $\gamma = 0.1$. The images recovered using the MS and MSTV stabilizers are shown bottom-left and bottom-right respectively. In these cases the parameters were $\alpha = 0.5$ and $\epsilon = 0.1$, with $\beta = 2.2$ for MS and $\beta = 1.5$ for MSTV.

The images recovered with MS and MSTV regularization are quite similar and visibly cleaner than the image obtained using the Beltrami flow stabilizer. Fig. 3 shows magnifications of the images obtained with Beltrami (left) and MSTV (right) regularization. The quantitative PSNR results are shown in the right column of Table 1, and are compatible with the perceived visual quality.

The superiority of the MS and MSTV regularizers with respect to the Beltrami flow in dealing with impulse noise can be well understood via the robust statistics interpretation presented in section 4. While all three stabilizers support inter-channel coupling, only the MS and MSTV methods impose an edge organization constraint. Edge organization is at the heart of the difference between an impulse noise point and a point that is part of a structured image edge.

The robust statistics perspective can be also used to compare the MS and MSTV regularizers. Fig. 4 presents the robust functions corresponding to the MS regularizer (solid, red) and the MSTV stabilizer at two values of γ. The dotted (green) curve corresponds to $\gamma = 0.1$ that we used in our experiments, and the dashed (blue) curve is for $\gamma = 10^{-10}$. The solid and dotted curves nearly coincide near the origin, but elsewhere the MSTV curve is lower than the solid curve. This implies better edge preservation with the MSTV regularizer. As γ is decreased, the MSTV robust function becomes narrower, driving the recovered

Fig. 2. Color image restoration using several regularization methods. *Top-left:* Blurred image with 30% impulse noise. *Top-right:* Beltrami flow regularization. *Bottom-left:* Color Mumford-Shah (MS). *Bottom-right:* Color TV Mumford-Shah (MSTV).

image towards the cartoon (piecewise constant) limit. Additional insight about the importance of color-channel coupling in image restoration can be gained by comparing restoration using multi-channel MS regularization with channel-by-channel MS restoration, i.e., by applying the method of [15] to each channel separately. As seen in Fig. 5, the multi-channel approach yields excellent results even at a high (40%) level of impulse noise (left), where channel-by-channel processing is clearly inadequate.

Finally, a useful byproduct of the MS and MSTV regularization methods is the auxiliary function v, that can serve as an edge map. Fig 6 (left) is a blurred and noisy *Lena* image; Fig 6 (right) is the v function (edge map) obtained with the MS regularizer.

6   Conclusion

We presented variational methods for color image deblurring with impulse noise. The methods share an L^1 color fidelity term, but differ in the regularization used. Our results verify the importance of channel coupling in the regularization terms. Furthermore, with impulsive noise, regularization methods based on
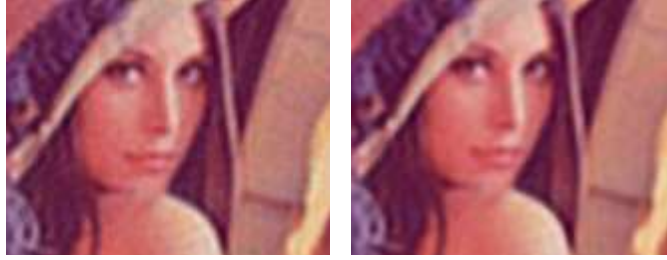
Fig. 3. Magnification of the images shown in the right column of Fig. 2. *Left:* Beltrami flow regularization. *Right:* MSTV regularization.
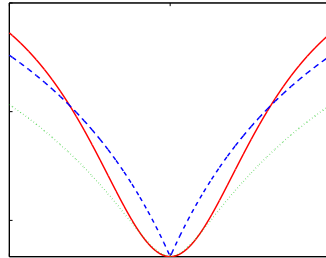
Fig. 4. Robust functions. *Red solid:* ρ^{MS}. *Blue dashed:* ρ^{MSTV} with $\gamma = 10^{-10}$. *Green dotted:* ρ^{MSTV} with $\gamma = 0.1$.

the Mumford-Shah functional and its variants are superior to other methods, including the Beltrami flow. This is seen in the experiments, and theoretically explained from the robust statistics point of view. Promising deconvolution results are obtained even at high levels of impulsive noise.

Acknowledgment

References

1. Tikhonov, A.N., Arsenin, V.I.: Solutions of ill-posed problems. Winston (1977)
2. Rudin, L., Osher, S., Fetami, E.: Non linear total variatrion based noise removal algorithms. Physica D **60** (1992) 259–268
3. Nikolova, M.: A variational approach to remove outliers and impulse noise. J. Math. Imaging Vision **20** (2004) 99–120
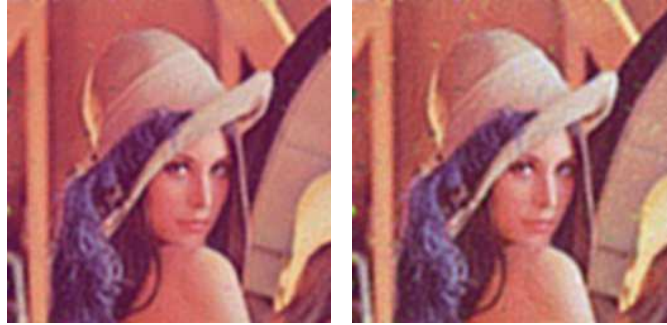
Fig. 5. Multi-channel vs. chanel-by-channel deblurring at a high level of impulse noise (40%). *Left:* Multi-channel MS regularization. *Right:* Channel-by-channel MS processing.

Fig. 6. *Left:* Blurred image contaminated by 30% impulsive noise. *Right:* Edge map obtained as a by-product of restoration using MS regularization.

4. Nikolova, M.: Minimizers of cost-functions involving nonsmooth data-fidelity terms: Application to the processing of outliers. SIAM J. Numer. Anal. **40** (2002) 965–994
5. Deriche, R., Faugeras, O.: Les EDP en traitement des images et vision par ordinateur. Traitement du Signal **13** (1996)
6. Welk, M., Theis, D., Brox, T., Weickert, J.: PDE-based deconvolution with forward-backward diffusivities and diffusion tensors. In: Proceeding of 5th International Conference on Scale Space and PDE Methods in Computer Vision. Volume 3439 of LNCS. (2005) 585–597
7. Bar, L., Sochen, N., Kiryati, N.: Variational pairing of image segmentation and blind restoration. In Pajdla, T., Matas, J., eds.: Proceedings of 8th European Conference on Computer Vision. Volume 3022 of LNCS. (2004) 166–177
8. Blomgren, P., Chan, T.F.: Color TV: total variation methods for restoration of vector-valued images. IEEE Trans. Image Processing **7** (1998) 304–309
9. Barash, D.: One-step deblurring and denoising color images using partial differential equations. Technical Report HPL-2000-102R1, HP Laboratories (2000)

10. Perona, P., Malik, J.: Scale-space and edge detection using anisotropic diffusion. IEEE Trans. Pattern Anal. Mach. Intell. **12** (1990) 629–639
11. Kaftory, R., Sochen, N., Zeevi, Y.Y.: Color image denoising and blind deconvolution using the Beltrami operator. In: Proceedings of the 3rd International Symposium on Image and Signal Processing and Analysis. Volume 1. (2003) 1–4
12. Hunt, B., Kübler, O.: Karhunun-Loeve multispectral image restoration, part I: Theory. IEEE Trans. Acoustics, Speech and Signal Proc. **32** (1984) 592–600
13. Banham, M., Katsaggelos, A.: Digital image restoration. IEEE Signal Processing Mag. **14** (1997) 24–41
14. Molina, R., Mateos, J., Katsaggelos, A.K., Vega, M.: Bayesian multichannel image restoration using compound Gauss-Markov random fields. IEEE Trans. Image Proc. **12** (2003) 1642–1654
15. Bar, L., Sochen, N., Kiryati, N.: Image deblurring in the presence of salt-and-pepper noise. In: Proceeding of 5th International Conference on Scale Space and PDE Methods in Computer Vision. Volume 3439 of LNCS. (2005) 107–118
16. Brook, A., Kimmel, R., Sochen, N.: Variational restoration and edge detection for color images. J. Math. Imaging Vision **18** (2003) 247–268
17. Sochen, N., Kimmel, R., Malladi, R.: A general framework for low level vision. IEEE Trans. Image Proc. **7** (1998) 310–318
18. Tschumperlé, D.: PDE's based regularization of multivalued images and applications. PhD thesis, University of Nice–Sophia Antipolis (2002)
19. Kimmel, R., Malladi, R., Sochen, N.: Images as embedded maps and minimal surfaces: Movies, color, texture, and volumetric medical images. Int. J. Computer Vision **39** (2000) 111–129
20. Mumford, D., Shah, J.: Optimal approximations by piecewise smooth functions and associated variational problems. Comm. Pure Appl. Math. **42** (1989) 577–685
21. Ambrosio, L., Tortorelli, V.M.: Approximation of functionals depending on jumps by elliptic functionals via Γ-convergence. Comm. Pure Appl. Math. **43** (1990) 999–1036
22. Shah, J.: A common framework for curve evolution, segmentation and anisotropic diffusion. In: IEEE Conference on Computer Vision and Pattern Recognition. (1996) 136–142
23. Alicandro, R., Braides, A., Shah, J.: Free-discontinuity problems via functionals involving the L^1-norm of the gradient and their approximation. Interfaces and Free Boundaries **1** (1999) 17–37
24. Strong, D., Chan, T.: Edge-preserving and scale dependent properties of total variation regularization. CAM Report 00–38, UCLA Math department (2000)
25. Vogel, C.R., Oman, M.E.: Fast, robust total variation-based reconstruction of noisy, blurred images. IEEE Trans. Image Proc. **7** (1998) 813–824
26. Charbonnier, P., Blanc-Féraud, L., Aubert, G., Barlaud, M.: Deterministic edge-preserving regularization in computed imaging. IEEE Trans. Image Proc. **6** (1997) 298–311
27. Geman, S., McClure, D.E.: Bayesian image analysis: An application to single photon emission tomography. Proc. Amer. Statist. Assoc. Statistical Computing Section (1985) 12–18
28. Teboul, S., Blanc-Féraud, L., Aubert, G., Barlaud, M.: Variational approach for edge-preserving regularization using coupled PDE's. IEEE Trans. Image Proc. **7** (1998) 387–397